Proceedings of the Twenty-seventh (2017) International Ocean and Polar Engineering Conference **www.isope.org**
San Francisco, CA, USA, June 25-30, 2017

ISBN 978-1-880653-97-5; ISSN 1098-6189

Numerical Study of Oscillatory Dual Cylinders in Tandem Arrangement

Xiaotong Zhang[1], *Dixia Fan*[2], *Decheng Wan*[1*]
[1] Collaborative Innovation Center for Advanced Ship and Deep-Sea Exploration, State Key Laboratory of Ocean Engineering, School of Naval Architecture, Ocean and Civil Engineering, Shanghai Jiao Tong University, Shanghai, China
[2] Department of Mechanical Engineering, Massachusetts Institute of Technology, Cambridge, MA, USA
[*]Corresponding author

ABSTRACT

In this paper, two-dimensional numerical study of dual cylinders with tandem arrangement undergoing sinusoidal oscillation in still water at a relatively low Reynolds number of 200 is conducted with overset grid technique in our solver pimpleDyMFoam-os, which is developed on the basis of open source code OpenFOAM to remain high mesh quality in spite that objects are performing large amplitude motion. Mesh dependent study and model validation are achieved firstly focusing on cases with single cylinder and tandem dual cylinders, where drag coefficients and added mass coefficients are taken into consideration to validate the accuracy of the solver as well as overset grid technique. As for cases with tandem dual cylinders, gap ratios (G/D, where G means gap between two cylinders and D represents diameter of each cylinder) are set as 0.5 and 1.0; Keulegan-Carpenter (*KC*) numbers are from 5 to 20 with an interval of 2.5, and β numbers are adjusted according to Reynolds Numbers and *KC* numbers. Drag coefficient and added mass coefficient are obtained with least square method. Moreover, strongly asymmetrical wake about the center line has been clearly observed in some cases with large motion amplitude, hence RMS value of non-dimensional lift force perpendicular to direction of forced motion is calculated to evaluate the degree of wake asymmetry, and its reasonability has been validated to some extent. Moreover, when the gap ratio is small with tandem dual cylinders, the block effect of the gap is strong and the wakes of after each cylinder tend to connect and finally become a union large vortex pair. This vortex pair and the block effect induce wakes to be symmetrical. Thus development of this unique characteristic in time domain and interaction between wakes of each cylinder are deeply analyzed and discussed.

KEY WORDS: Tandem dual cylinders; Oscillatory flow; RMS value; Wake analysis; naoe-FOAM-os-SJTU solver.

INTRODUCTION

Cylinders in oscillatory flow have been attracting extensive concern due to its significant scientific contribution to people's understanding on mechanism of vortex and its wide spread in engineering field after reasonable simplification since water particle trajectories near seabed are nearly cyclic circular motion. The in-line force on a cylinder in oscillatory flow agrees with Morison Equation, and a linear sum of the drag forces and inertial forces per unit length are just shown as the following Eq. 1.

$$F_{in-line} = \frac{1}{2}\rho D C_d |U| U + \frac{1}{4}\pi\rho D^2 C_m \frac{dU}{dt} \quad (1)$$

where C_d and C_m are the drag coefficient and inertia coefficient respectively. And they can be easily separated from the total in-line force with the method of least-square method or Fourier averaging based on the in-line force time series. However, no matter in the experiments or numerical simulations, it is difficult to control the velocity distribution along the boundary of the tank or calculation domain to be harmonic. Thus it is reasonable to force the circular cylinder to perform sinusoidal oscillation in still water to simplify the experimental and numerical arrangement. And the main difference when compared with results of fixed circular cylinder in oscillatory flow is that the cylinder will experience Froude-Krylov force when fixed in oscillatory flow due to the pressure gradient along the oscillation period. As the inertia coefficient in Morison Equation can be written as $C_m = 1 + C_a$, where C_a is added mass coefficient and 1 accounts for the Froude-Krylov force, the problems related to force coefficient can be easily dealt with. Thus, C_m in this paper is the inertia coefficient after adding 1. However, the vortex flow, the vortex shedding pattern and vortex structure are all the same in these two settings.

When a circular cylinder is positioned in viscous sinusoidal oscillatory flow, the hydrodynamic forces on the cylinder and flow field characteristics are mainly dependent on two parameters, namely Keulegan-Carpenter number (Keulegan & Carpenter, 1956) and Strokes number (Sarpkaya, 1976). *KC* numbers and Strokes numbers

(β) are defined as U_mT/D and $D^2/\nu T$ respectively, where U_m is the maximum oscillatory flow velocity, D is the diameter of the cylinders, T is the period of oscillatory flow and ν is the kinematic viscosity of fluid. In the meantime, Strokes number β can also be obtained by Re/KC, where Re is the Reynolds number defined by U_mD/ν. Williamson (1985a) identified various flow regimes based on the number of vortex pairs shed from the cylinder in a whole period with experimental methods. Tatsuno and Bearman (1990) further clarified the 8 different flow regimes (A*, A, B, C, D, E, F and G) with flow visualization experiments of *KC* from 1.6 to 15 and Strokes number from 5 to 160. A lot of other experimental or numerical investigations on this topic have been widely conducted, such as boundary layer separation, vortex shedding and flow reversal etc. (Iliadis and Anagnostopoulos, 1998; An, Cheng and Zhao, 2009; Hall, 1984; Elston, Sheridan & Blackburn, 2004).

The investigation in this paper is based on two-dimensional simulation which can make the phenomenon more clear and save most of the calculation time although the capability of computers and processors has been promoted significantly. Honji (1981) and Sarpkaya (1986) investigated the flow transition from 2-dimensional to 3-dimensional. And Sarpkaya (2002) proposed a criterion for critical *KC* number, above which the flow will become three-dimensional.

$$K_{cr}\beta^{2/5} = 12.5 \tag{2}$$

All the cases in this paper are below this critical *KC* number, thus 2-dimensional simulation can reduce computing time and make us focus more on phenomena themselves. Extensive numerical investigations on single circular cylinder in oscillatory flow have been conducted. Justesen (1991) performed two-dimensional simulation in the range of *KC* from 0.1 to 26 and β at 196, 483 as well as 1035. In his study, he discussed systematically about force coefficients, flow structures and pressure distribution. Saghafian, Stansb, Saidi and Apsley (2003) simulated the cases with high Strokes numbers by solving the two-dimensional Reynolds-Averaged Navier-Stokes (RANS) equations and the results agree quite well with the experimental results.

Compared with single circular cylinder, investigation on problems about dual circular cylinders in oscillatory flow is relatively rare. Williamson (1985b) discovered that wakes after two side-by-side cylinders are just like a single circular cylinder when gap ratios are less than 1.2. Chern, Kanna, Lu, Cheng and Chang (2010) focused on side-by-side configuration and found that gap ratios has a major effect on vortex shedding pattern and the vortex shed from the cylinders are symmetrical with *KC* less than 10. Zhao and Cheng (2014) undertook 2-dimensional simulation on both side-by-side and tandem arrangement. And they found that in tandem arrangement, when the gap ratios and *KC* numbers are small, the flow structures are just like a single cylinders. The flow with both side-by-side and tandem arrangement is irregular when *KC* is quite large. Furthermore, Tong, Cheng, Zhao and An (2015) carried out simulations about four-cylinder array in oscillatory flow. They figured out there are quite different flow characteristics when compared with two cylinders or single cylinder. However, we can see that the investigation on problems of tandem arrangement is quite limited.

Moreover, in recent decades, more and more numerical methods have been proposed in CFD to better solve large motion and complex geometries in the calculation domain. And they are applied quickly to this problem. Chern, Shiu and Horng (2013) applied a direct-forcing immersed boundary method to simulate the oscillatory flow past a circular cylinder array in square arrangement, and they also investigated the effects of *KC* number, oblique flow and gap among four cylinders to hydrodynamic loadings including in-line force and transverse force coefficients in both time and spectral domains. Harimi and Saghafian (2012) used overset grid method to study the fluid flow and forced convection heat transfer from tandem circular cylinders and the results can agree quite well with results from experiments and other simulations. Overset grid is quite a powerful tool on multiple hydrodynamic problems, such as computations for flows around a stationary cylinder with high Reynolds numbers by Ye and Wan (2016), unsteady aerodynamic simulations of floating offshore wind turbines by Cheng, Wan and Hu (2016), self-propulsion Simulation of ONR Tumblehome by Wang, Liu and Wan (2015) as well as Wang, Zhao and Wan (2016). In this paper, Overset Grid Technics are implemented to solve the problems brought up by large deformation. Moreover, tandem arrangement is mainly focused on and systematic discussion about the flow characteristics and force coefficient will be carried out with Overset Grid Technics. Moreover, a mesh dependent study and validation of numerical methods will also be conducted.

NUMERICAL METHODS

The solver used in this paper is naoe-FOAM-os-SJTU, our in-house code developed using open source CFD tool package OpenFOAM. And the postfix "os" is the abbreviate of Overset, which means Overset Grid Technics is integrated into original solver to accomplish complex or large-amplitude motion. naoe-FOAM-SJTU is a reliable code to solve unsteady incompressible problems, which has been validated for aerodynamics simulation of wind turbines by Zhou and Wan (2015). This time, Overset Grid Technique are combined with it and they are good choices for discussion of dual cylinders in oscillatory flow as large-amplitude motion may appear and normal dynamics mesh is quite hard to be dealt with when the gap ratio is small.

Governing Equations

For transient, incompressible and viscous fluid, flow problems are governed by non-dimensionalized Navier-Stokes equations in this paper. All the parameters are non-dimensionalized as $(x,y) = (x',y')/D$, $(u,v) = (u',v')/U_m$, $p = p'/\rho U_m^2$, and $t = U_mt'/D$. Where (x,y) are the point in Cartesian coordinates, (u,v) are the velocity component in x and y direction respectively, t is time, p is pressure, ρ is the density of the fluids, U_m is the maximum velocity of the cylinder's forced motion. Thus the non-dimensional Navier-Stokes equations can be expressed as following Eq. 3:

$$\begin{aligned}
&\frac{\partial u}{\partial t} + u\frac{\partial u}{\partial x} + v\frac{\partial u}{\partial y} + \frac{\partial p}{\partial x} - \frac{1}{Re}\nabla^2 u = 0,\\
&\frac{\partial v}{\partial t} + u\frac{\partial v}{\partial x} + v\frac{\partial v}{\partial y} + \frac{\partial p}{\partial y} - \frac{1}{Re}\nabla^2 v = 0,\\
&\frac{\partial u}{\partial x} + \frac{\partial v}{\partial y} = 0,
\end{aligned} \tag{3}$$

where *Re* is Reynolds number. And all the following discussion are based on this non-dimensional method and expression unless specially indicated.

Overset Grid Technique

Overset grid technique allows multiple overlapping grids for different part of objects with separate motion. The connection among grids is accomplished by interpolation at appropriate cells or point using DCI (Domain Connectivity Information). Firstly, SUGGAR++ will mark the hole cells which are located outside simulation domain or the area where we are of no interest. And the code can easily exclude them from computation. Fig.1 shows the diagram of overset grids, and we can see that there are several cells around hole cells named fringe cells, and there are also several donor cells providing information for fringe cells.

Then the code is going to find the donor cells for each fringe cells and send information from donor cells to fringe cells.

Next, a variable ϕ of fringe cells is obtained by interpolation using following equation from its own donor cells.

$$\phi_I = \sum_{i=1}^{n} \omega_i \cdot \phi_i \tag{4}$$

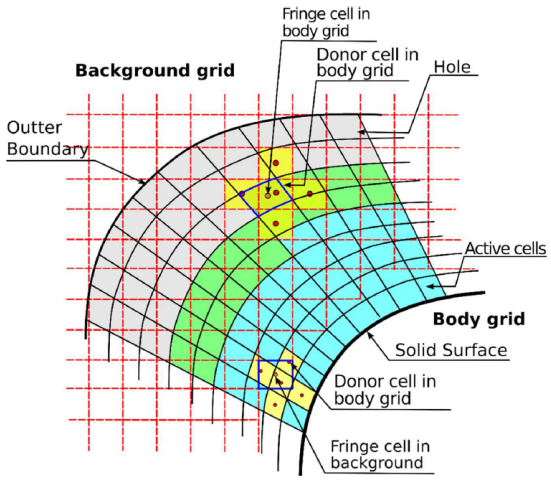

Fig. 1 Diagram of overset grids (from website source)

Next, a variable ϕ of fringe cells is obtained by interpolation using following equation from its own donor cells.

$$\phi_I = \sum_{i=1}^{n} \omega_i \cdot \phi_i \tag{5}$$

where ϕ_I is the value of variable ϕ of the fringe cell, ϕ_i is the value for the i_{th} donor cell, ω_i is the weight coefficient, which is dimensionless and satisfies the following equation.

$$\sum_{i=1}^{n} \omega_i = 1 \tag{6}$$

And finally, the overlapping area will be optimized and accuracy of interpolation will be improved.

NUMERICAL SIMULATION

The coordination system set in this paper is defined in Fig. 2. The cylinders are forced to oscillate together along x axis with the displacement expression of $X(t) = Asin(\omega t)$. The direction of in-line force is also in *x-axis*, while lift force is in the direction of y.

In this paper, we are going to simulate the cases with gap ratio of 0.5 and 1.0 for tandem dual cylinders, as gap ratio means Gap/Diameter. For each arrangement including single cylinder arrangement, KC numbers are 5.0, 7.5, 10.0, 12.5, 15.0, 17.5 and 20.0 respectively. Reynolds number in all cases are set to be a fixed number of 200. Then Strokes number are adjusted according to KC numbers and Reynolds numbers with the relationship that β=Re⁄KC. The time step in all cases are the same and relatively small to confirm that courant numbers are less than 1.0 in the whole calculation time.

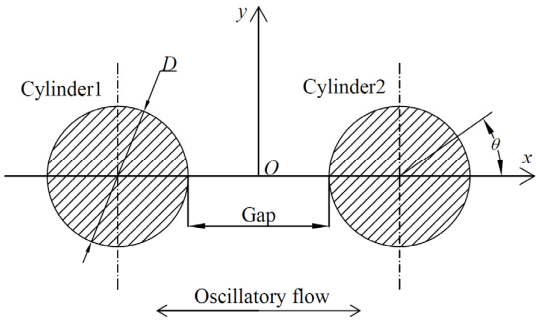

Fig. 2 Coordinate system for tandem cylinders with gap ratio of 1.0

Mesh Dependent Study

With overset grid technique, we have to draw 2 sets of grids for single cylinder cases and 3 sets of grids for two cylinder cases separately for SUGGAR++ to interpolate, namely one mesh for each cylinder and one more mesh for background. We are going to conduct mesh dependent study firstly to determine the mesh refinement degree to balance the calculation time and accuracy. The mesh around and moving together with circular cylinder is also a circular mesh with a diameter of 3D (D means diameter) in all the cases. The main factor to influence more for each cylinder is Δr (minimum non-dimensional mesh size in the radial direction next to the cylinder surface), N_s (the number of nodes along the surface of circular cylinder) and N_n (the total node number in the mesh region). The background calculation domain is set to be 15D × 10D. Then the block coefficients in all cases are 10% to erase block effect. The background mesh is structured meshes composed of cubic cells of the same non-dimensional length and width which will be expressed as s. The parameters of the three sets of meshes are list in Table 1.

Table. 1 Mesh parameter

Mesh Density	Cylinder Mesh			Background Mesh	
	N_s	$N_{n\ c}$	Δr	s	$N_{n\ b}$
Coarse	72	2520	0.0030	0.15	20301
Normal	84	3780	0.0024	0.10	45451
Dense	112	5600	0.0016	0.08	71188

The cases in mesh dependent study are the cases of tandem cylinders with KC number of 5 and Re number of 100, where the vortex flow is in a regular and steady regime. The C_m and C_d coefficient of cylinder1 are calculated and compared here in Table 2. From the result, we can see that the difference between drag coefficients are so slightly that can be hardly detected. However, there are still some differences when comparing added mass coefficients. When the meshes become denser from coarse to normal, the relative difference is 0.25%, while the difference between results of dense mesh and normal mesh is 0.11%. However, the difference between cell numbers and calculation time is quite large, and the dense mesh cases need a much longer calculation time.

Table. 2 Comparison of force coefficient of cylinder1

Mesh	C_m	C_d
Coarse Mesh	2.1687	2.0386
Normal Mesh	2.1742	2.0384
Dense Mesh	2.1765	2.0383

The vorticity contour at non-dimensional time of 29.54 is shown in Fig. 3. In the figure, the difference of vortex flow between three meshes are

also very slightly. However, the vorticities of normal mesh and dense mesh are slightly stronger than coarse mesh, due to the dissipation of vortex when the mesh sizes are large, especially for the vortex pair A in the gap and vortex pair B. In the coarse mesh results, the gap vortex pair A can hardly be detected. The results of normal meshes and dense meshes agree with each other quite well. We can draw the conclusion that the difference between normal meshes and dense meshes will not greatly influence the vortex structure and vortex shedding pattern. However, the difference between cell number of meshes and calculation time is quite large. And the cases with dense meshes need nearly two times of calculation time of that with normal meshes. Thus in the following study, we will choose the normal meshes to balance the calculation time and simulation accuracy.

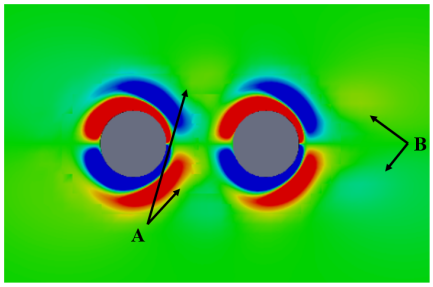

(a) Coarse

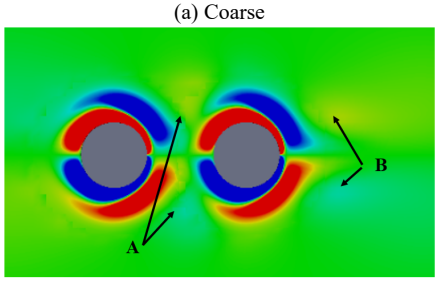

(b) Normal

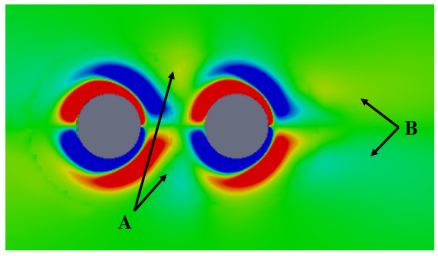

(c) Dense

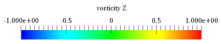

Fig. 3 Vorticity contour at non-dimensional time of 29.54

To better obtain the vortex shedding pattern of far flow field in some specific cases, we extend the calculation domain to $30D \times 20D$. The original area of meshes maintain the mesh density of normal meshes. And the mesh length of extended area is half of that in the original area. This will not influence the calculation accuracy of force acting on cylinders, but will provide us with a wider view of the vortex spreading. The final calculation domain and meshes for tandem cylinders with gap ratio of 1.0 is shown in figure 4(a). Moreover, the partial enlarged figure of near cylinder area is shown in Fig. 4(b), and the red region in Fig. 4 is the overset meshes for cylinders and it will move in the yellow part of background meshes to establish motion and interpolate with background information.

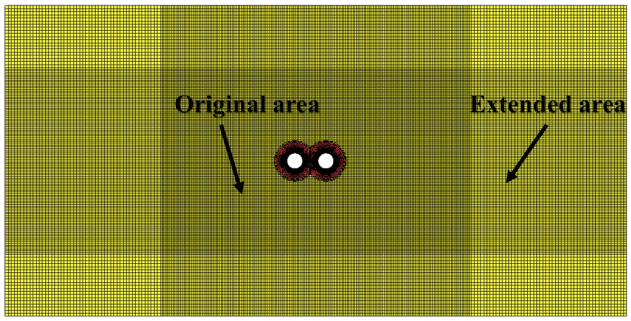

(a) Overall view of the calculation domain and meshes

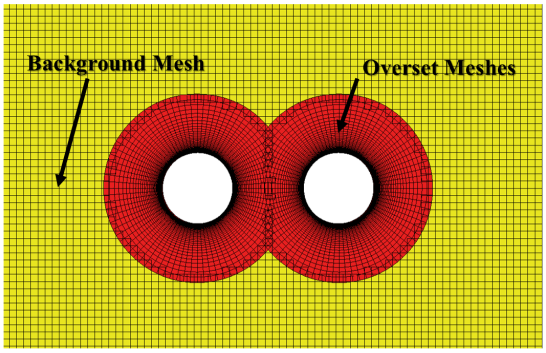

(b) Overset meshes of cylinders

Fig. 4 calculation domain and mesh

Model Validation

Various studies about problems of single cylinder has been carried out. Given that when *KC* is large, the force in each period also varies a lot, and the flow structure turns to be irregular, thus a case with small *KC* number of 5 and *Re* number of 100 has been put forward to compare the results with different solvers and methods to validate the numerical model in this study. The same cases has been simulated by Dütsch, Durst, Becker and Lienhart (1998) on low-Reynolds-number simulation; Nehari, Armenio and Ballio (2004) on both two-dimensional and three-dimensional study; Uzunoglu, Tan and Price (2001) with a cell viscous boundary element method; Zhao and Cheng (2014) with fixed cylinder and oscillatory flow velocity boundary. In the validation, our cases are simulated with overset grid technique, and our results as well as results from other studies are all shown in Table 3.

Table. 3 Comparison of force coefficient for oscillatory flow past a circular cylinder (*KC*=5, *Re*=100)

Source	C_m	C_d
2D numerical result (Dütsch et al. 1998)	2.45	2.09
2D numerical result (Nehari et al. 2004)	2.43	2.10
2D numerical result (Uzunoglu et al. 2001)	2.45	2.10
2D numerical result (Zhao et al. 2004)	2.48	2.04
3D numerical result (Nehari et al. 2004)	2.47	2.13
Present with overset grid technique	2.43	2.09

From the results in Table. 3, we could see that our results show a quite good agreement with other people's results. The added mass coefficient is the same with Nehari, Armenio and Ballio (2004), but their results as well as ours are a little smaller than other people's results. As for drag coefficients, Zhao and Cheng (2014)'s results are the least, however Nehari, Armenio and Ballio (2004)'s 3-D results are the largest, while our results are between them and nearly the same with Dütsch, Durst,

Becker and Lienhart (1998)'s results. However, these results are quite close and it will show not significant influence to the following investigation. Thus, our numerical models, numerical methods as well as the utility of overset grid technique are all validated. This is quite important to provide more accurate numerical results and reference for others and it also serves as a basic work for the upcoming further study about problems of dual cylinders in tandem arrangement.

Dual Cylinders in Tandem Arrangement

Investigation about dual cylinders in oscillatory flow has been widely studied, however, the understanding related to tandem configuration is still quite rare. To better analyze the influence between wakes of two cylinders, the added mass coefficient and drag coefficient of dual cylinders, with gap ratio of 0.5 and 1.0, and single cylinders are shown in the Fig. 5. All the results in this paper are calculated based on data of more than 60 periods excluding the initial 20 periods that the vortex flow has not developed fully. As for cases with dual cylinders, we calculate both C_m and C_d of two cylinders, but the results are quite the same. Thus we will choose results of cylinder1 as the results of this configuration.

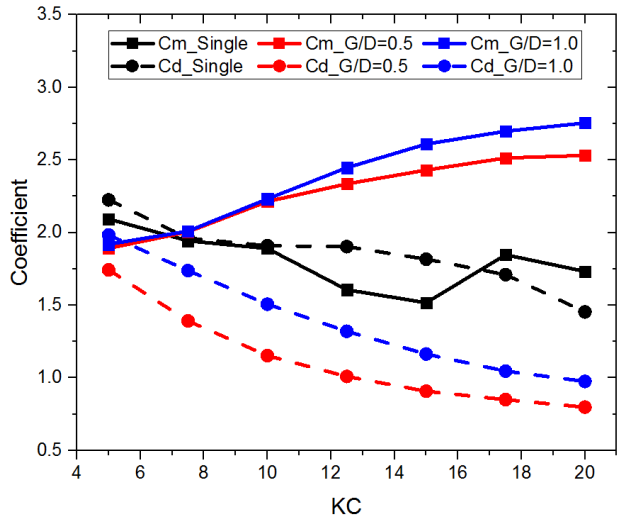

Fig. 5 C_m and C_d vs. *KC* numbers (Gap ratio=0.5/1.0 and single)

As for the single cylinder cases in Fig. 5, C_m and C_d coefficients under different *KC* show various trends and it is more complex compared with dual cylinders in tandem arrangement. The C_m of single cylinder firstly decreases with the increase of *KC* and then enhances at *KC* of 17.5 and finally drops again at *KC* of 20. A pure trend is impossible to draw due to the transition of vortex shedding pattern. However, the drag coefficient shows a monotone decreasing trend from 2.22 to 1.45 despite the wake regime transits over *KC* numbers. Moreover, when *KC* is quite large, the flow regime turns out to be more irregular, thus C_m and C_d will depend more on the time used to calculate the results.

As for dual cylinders with gap ratio of 0.5 and 1.0 in Fig. 5, the trends are quite simple and we can draw a monotone trend that C_m increases and C_d decreases with increase of *KC* numbers. And the two drag coefficient lines are just like the same line after translation. However, the drag coefficient of gap ratio of 1.0 is much larger than that of gap ratio of 0.5. While the C_m of gap ratio of 0.5 and 1.0 for small *KC* number is nearly the same and the difference begins to increase from *KC* number of 10.0. Given that drag force is the dissipative force, while added mass force is conservative force, large drag coefficient means that the energy is easier to dissipate from structure to flow field, and the flow field will be much messier, which can also be of great engineering significance. The trends of C_m and C_d with gap ratio of 0.5 and 1.0 are quite the same and it is different from that of single cylinder, which means the interaction between wakes after two cylinders is quite strong, and it is going to induce some locked phenomenon that will not be broken until the gap ratio is large enough.

Moreover, the force on the cylinders is the reflection of the flow field and the lift force is induced by the asymmetrical wake and unbalanced pressure on the cylinder surface. Thus the RMS of non-dimensional lift force (simplified as RMS in the rest of the paper) is calculated and it is defined as the Eq. 7 shows.

$$\mathrm{RMS} = \sqrt{\frac{\sum(Force_y{}^2)}{N}} \tag{7}$$

where $Force_y$ is the non-dimensional lift force in the direction of y and defined as $Force_y = F_y/(0.5\rho U_m^2 S)$, N is the total number of data point of $Force_y$. With this definition, RMS is useful to evaluate the rate of asymmetry, and it is shown in the Fig. 6 for single cylinder as well as gap ratio of 0.5 and 1.0.

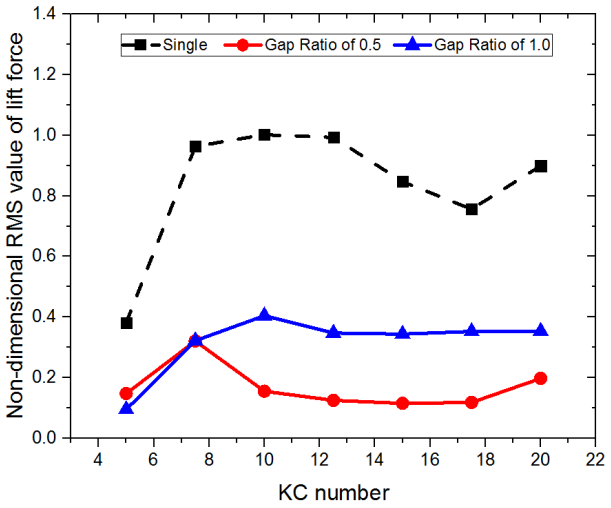

Fig. 6 RMS vs. *KC* number for different configuration

We could see that the RMS of single cylinder is going to greatly increase at *KC* of 7.5 and when *KC* is 5, the RMS is quite low to show a nearly symmetrical flow. And then it drops at *KC* of 17.5, which relates to vortex shedding pattern and flow regime transition, just like the trends of C_m and C_d of single cylinder cases. The vortex structure and shedding pattern at *KC* of 5 and 7.5 are illustrated in Fig. 7. The vorticity in this paper is also non-dimensional and calculated from non-dimensional velocity and with equation of $\omega = \partial v/\partial x - \partial u/\partial y$. The vortex shedding pattern in Fig. 7(a) is in a classical regime A, that two vortices shed symmetrically per half period defined by Tatsuno and Bearman (1990). While, in Fig. 7(b) for *KC* of 7.5, the cylinder is moving leftwards. The vortex pair A sheds in last half period and vortex pair B sheds in this half period. The positive upper vortex of B is going contribute to the large vortex C. Thus the left part of wake is in regime D, while the right part shows the characteristics of regime C at this time, but both regimes C and D are asymmetrical. And the RMS value increases from 0.38 at *KC* of 5 to 0.96 at *KC* of 7.5.

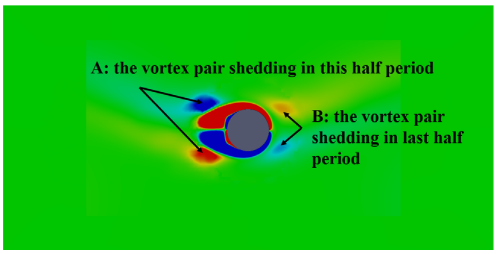

(a) *KC* of 5 at time of 143.07
(non-dimensional time, the same as following)

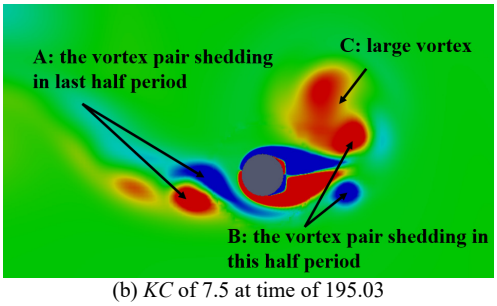

(b) *KC* of 7.5 at time of 195.03

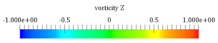

Fig. 7 vortex contour of single cylinder (Re of 200)

Moreover, we could see in Fig. 6 that when *KC* is larger, the RMS values of dual cylinders are less than those of single cylinder, and it can also be reflected in the vortex contour for three configuration under *KC* of 17.5, which is shown in Fig. 8. In Fig. 8, we could clearly see that the degree of asymmetry shows good agreement with RMS value. In Fig. 8(a), the single cylinder will shed one vortex pair A in a half period and the vortex flow is in regime F, which is a regime with flow convected diagonally. And the vortex pair B is the vortex pair shedding in last half periods. The vortex structure is still irregular, and the vortex will be a little different beyond each half period. However, it remains in flow regime of F for a quite long time and we could see that the rate of asymmetry is quite strong and it will greatly influence the lift force as the vortex is in the direction of diagonal. When it comes to dual cylinders with gap ratio of 0.5, the left-handed cylinder1 sheds the vortex pair A, and the right-handed cylidner2 sheds the vortex pair B. Due to neutralization of main wake of cylidner2, the vortex A is quite weak and only a little part of it can be shed into the background. However, the wake is quite symmetrical compared with other configuration. When the gap ratio increases to 1.0, which is shown in Fig. 8(c), the wake after two tandem cylinders is nearly with the same pattern like that in Fig. 8(b). However, as the interaction between two cylinders are going to be weaker, the effect that makes the wake symmetrical and act like a single cylinder also becomes weaker. Thus it makes that the vortex wakes are going to resemble the wake of single cylinder, and it is more asymmetrical than gap ratio of 0.5, and one more vortex shedding is discovered in each half period. In the Fig. 8(c), there is an additional vortex C shedding from the upper sides of cylinder2 besides the vortex pair A from cylinder1 and B from cylinder2, which is almost symmetrical when gap ratio is 0.5. The single vortex C greatly enhances the rate of asymmetry and further greatly influences the vortex field. At *KC* of 17.5, the RMS value of single is the largest, the second one is gap ratio of 1.0; and the least is gap ratio of 0.5, which shows an almost symmetrical wake. Thus it is reasonable to evaluate the degree of asymmetry in the vortex wake with RMS value of lift force.

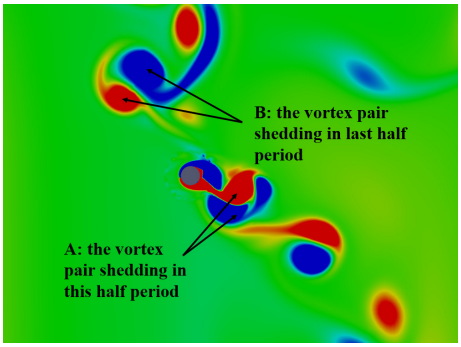

(a) single cylinder

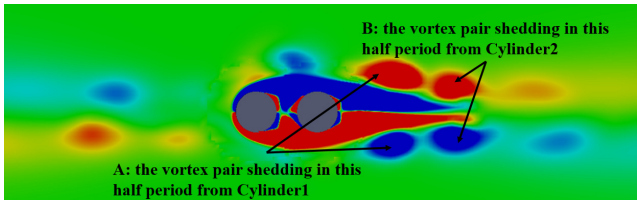

(b) gap ratio of 0.5

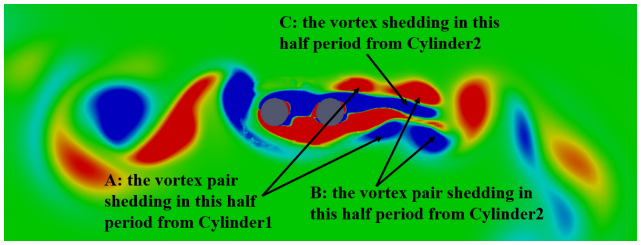

(c) gap ratio of 1.0

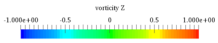

Fig. 8 Vortex contour for different configuration at *KC* of 17.5 and time of 100.56 (Re of 200)

The phenomenon, that dual cylinders in tandem arrangement with small gap ratio of 0.5 and 1.0 forms wakes in regime A and A* at low *KC* number and regime D at large *KC* numbers, is also discovered in Zhao and Cheng (2014)'s results at Reynolds number of 150. In our results, the flow is also in regime D at gap ratio of 1.0, while in regime A at gap ratio of 0.5 as shown in Fig. 8(b). However, there are still some phenomena in regime D shown in different half periods as we have previously discussed that when *KC* is large, the flow tends to be irregular in different half periods. Thus our results also agree well with Zhao and Cheng (2014)'s results. However, the single cylinder with the same *KC* number is in regime F and the wake propagates in the direction of diagonal. Thus the interaction between the wakes of cylinders greatly changes the flow pattern. At gap ratio of 0.5, the development of the wakes after two cylinders is illustrated in Fig. 9. When the cylinders get to the left largest displacement, the wake of each cylinder is shown in Fig 9(a), and vortex A and B are the vortex of cylidner1 and cylidner2 in next half period, but has already been generated, separately. And vortex group C is the vortex of cylinder1 and cylidner2 that shed in last half periods. The vortex pair A and B are just like the vortex of single cylinder, which is generated near the largest displacement point and need further development. Then the cylinders are going to reverse and moving leftwards in Fig. 9(b). Vortex A and B further develop to become bigger, longer and stronger.

In the meantime, the longer vortex wake of A and B connect with each other and the connection becomes stronger. And finally vortex A and B become a new union vortex D and it encircles cylinder1 and cylinder2. In Fig. 9(a), the wake A and B are just like that of single cylinder, but with the influence of cylinder2, vortex A tends to cylinder2 and well connects with vortex B. The influence of B to A is just like a "magnet" to attract vortex A to B and finally becomes symmetrical due to the existence of cylinder2. However, as the gap ratio increases to quite large, like 3.0 or 4.0, the "magnet" effect of cylinder2 to wake of cylinder1 is going to be weaker, and the wake turns out to be more complex as the wakes of two cylinders may not merge, but even be stirred and make the flow field just a mess. Just like what we talked before, when the gap ratio increases to 1.0, the flow fields tend to be more complex, and three vortices will be shed in each half period. And we can easily observe that the vortex A of cylinder1 needs more time to connect with vortex B from cylinder2, and the connection between vortex A and B are quite weak, as shown in Fig 8(c). In Fig 8(b,c), we could see that the vortex A also tends to become asymmetrical due to the large motion amplitude, however, the small gap restricts the asymmetry from developing in space domain. But when gap ratio is 1.0, the larger gap permits the trend to asymmetry to develop more. When vortex A reaches vortex B, the vortex A performs asymmetrical influence to cylidner2 and vortex B. Moreover, the part of vortex C shed from cylinder1 is also asymmetrical, which accelerates the development of asymmetry. Thus, Cylinder2 sheds an additional asymmetrical vortex and results in the flow regime of E.

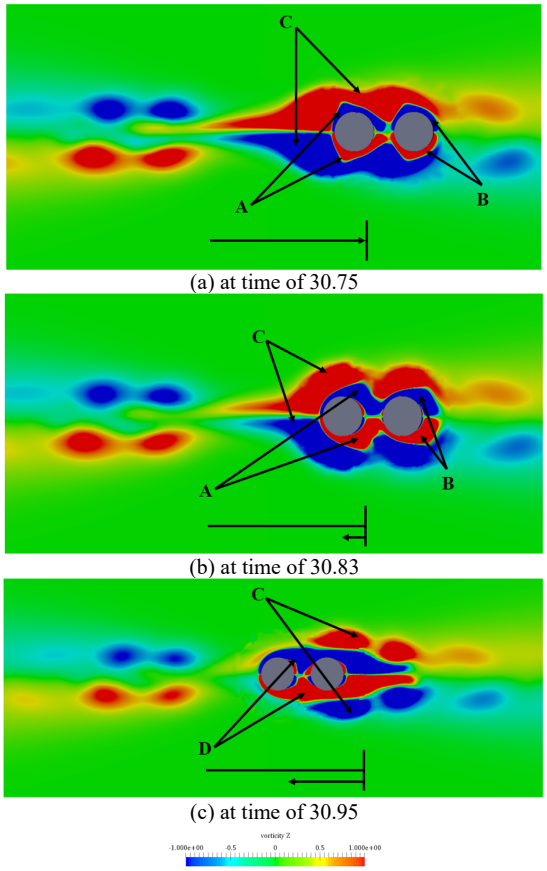

(a) at time of 30.75

(b) at time of 30.83

(c) at time of 30.95

Fig. 9 vortex development with tandem cylinders (gap ratio=0.5, *KC*=17.5, Re=200)

CONCLUSIONS

In this paper, we mainly focus on dual cylinders in tandem configuration, of course as well as single configuration to make a comparison to better analyze the interaction of wakes after two cylinders. We firstly conduct mesh dependent study and model validation, and our meshes can accurately simulate the problems of cylinders in viscous oscillatory flow and the results show good agreement with other people's numerical results. Then we calculate the C_m and C_d of cases in this study, and we find that the coefficient of tandem cylinders with small gaps shows a monotone trend vs *KC* numbers, while coefficients of single cylinders fluctuate severely due to the vortex shedding mode transition. Next we validate the reasonability of using RMS values to evaluate the degree of asymmetry with some specific cases. However, the RMS value of lift force also depends on other factors, not only on asymmetry, thus RMS value can only reflect degree of asymmetry to some extent. Finally, we analyze the vortex development in time domain and we discover that vortex B has a "magnet" effect to vortex A. And the gap has a significant influence of restriction on the development of asymmetry and transition of vortex shedding pattern.

ACKNOWLEDGEMENTS

This work is supported by the National Natural Science Foundation of China (51379125, 51490675, 11432009, 51579145), Chang Jiang Scholars Program (T2014099), Shanghai Excellent Academic Leaders Program (17XD1402300), Shanghai Key Laboratory of Marine Engineering (K2015-11), Program for Professor of Special Appointment (Eastern Scholar) at Shanghai Institutions of Higher Learning (2013022), Innovative Special Project of Numerical Tank of Ministry of Industry and Information Technology of China (2016-23/09) and Lloyd's Register Foundation for doctoral student, to which the authors are most grateful.

REFERENCES

An, H., Cheng, L., & Zhao, M. (2009). Steady streaming around a circular cylinder in an oscillatory flow. Ocean Engineering, 36(14), 1089-1097.

Cheng, P., Wan, D. C., & Hu, C. (2016, June). Unsteady Aerodynamic Simulations of Floating Offshore Wind Turbines with Overset Grid Technology. In The 26th International Ocean and Polar Engineering Conference. International Society of Offshore and Polar Engineers.

Chern, M. J., Kanna, P. R., Lu, Y. J., Cheng, I. C., & Chang, S. C. (2010). A CFD study of the interaction of oscillatory flows with a pair of side-by-side cylinders. *Journal of Fluids and Structures*, 26(4), 626-643.

Chern, M. J., Shiu, W. C., & Horng, T. L. (2013). Immersed boundary modeling for interaction of oscillatory flow with cylinder array under effects of flow direction and cylinder arrangement. *Journal of Fluids and Structures*, 43, 325-346.

Dütsch, H., Durst, F., Becker, S., & Lienhart, H. (1998). Low-Reynolds-number flow around an oscillating circular cylinder at low Keulegan–Carpenter numbers. *Journal of Fluid Mechanics*, 360, 249-271.

Elston, J. R., Sheridan, J., & Blackburn, H. M. (2004). Two-dimensional Floquet stability analysis of the flow produced by an oscillating circular cylinder in quiescent fluid. European Journal of Mechanics-B/Fluids, 23(1), 99-106.

Justesen, P. (1991). A numerical study of oscillating flow around a circular cylinder. *Journal of Fluid Mechanics*, 222, 157-196.

Hall, P. (1984). On the stability of the unsteady boundary layer on a cylinder oscillating transversely in a viscous fluid. Journal of Fluid Mechanics, 146, 347-367.

Harimi, I., & Saghafian, M. (2012). Numerical simulation of fluid flow and forced convection heat transfer from tandem circular cylinders using overset grid method. *Journal of Fluids and Structures*, 28, 309-327.

Honji, H. (1981). Streaked flow around an oscillating circular cylinder. *Journal of Fluid Mechanics*, 107, 509-520.

Iliadis, G., & Anagnostopoulos, P. (1998). Numerical visualization of oscillatory flow around a circular cylinder at Re= 200 and *KC*= 20—an aperiodic flow case. Communications in numerical methods in engineering, 14(3), 181-194.

Keulegan, G. H., & Carpenter, L. H. (1956). Forces on cylinders and plates in an oscillating fluid. US Department of Commerce, National Bureau of Standards.

Nehari, D., Armenio, V., & Ballio, F. (2004). Three-dimensional analysis of the unidirectional oscillatory flow around a circular cylinder at low Keulegan–Carpenter and β numbers. *Journal of Fluid Mechanics*, 520, 157-186.

Saghafian, M., Stansby, P. K., Saidi, M. S., & Apsley, D. D. (2003). Simulation of turbulent flows around a circular cylinder using nonlinear eddy-viscosity modelling: steady and oscillatory ambient flows. *Journal of fluids and structures*, 17(8), 1213-1236.

Sarpkaya, T. (1976). Vortex shedding and resistance in harmonic flow about smooth and rough circular cylinders at high Reynolds numbers. Monterey, California. Naval Postgraduate School.

Sarpkaya, T. (1986). Force on a circular cylinder in viscous oscillatory flow at low Keulegan—Carpenter numbers. *Journal of Fluid Mechanics*, 165, 61-71.

Sarpkaya, T. (2002). Experiments on the stability of sinusoidal flow over a circular cylinder. *Journal of Fluid Mechanics*, 457, 157-180.

Tatsuno, M., & Bearman, P. W. (1990). A visual study of the flow around an oscillating circular cylinder at low Keulegan–Carpenter numbers and low Stokes numbers. *Journal of Fluid Mechanics*, 211, 157-182.

Tong, F., Cheng, L., Zhao, M., & An, H. (2015). Oscillatory flow regimes around four cylinders in a square arrangement under small KC and Re conditions. J Fluid Mech, 769, 298-336

Uzunoğlu, B., Tan, M., & Price, W. G. (2001). Low‐Reynolds‐number flow around an oscillating circular cylinder using a cell viscousboundary element method. *International Journal for Numerical Methods in Engineering*, 50(10), 2317-2338.

Wang, J., Liu, X., & Wan, D. C. (2015). Numerical prediction of free runing at model point for ONR Tumblehome using overset grid method. In Proceedings of CFD Workshop 2015 (pp. 383-388).

Wang, J., Zhao, W., & Wan, D. C. (2016) Free Maneuvering Simulation of ONR Tumblehome Using Overset Grid Method in naoe-FOAM-SJTU Solver. In Proceedings of 31st Symposium on Naval Hydrodynamics.

Williamson, C. H. K. (1985a). Sinusoidal flow relative to circular cylinders. *Journal of Fluid Mechanics*, 155, 141-174.

Williamson, C. H. K. (1985b). Evolution of a single wake behind a pair of bluff bodies. *Journal of Fluid Mechanics*, 159, 1-18.

Ye, H., & Wan, D. C. (2017). Benchmark computations for flows around a stationary cylinder with high Reynolds numbers by RANS-overset grid approach. Applied Ocean Research. http://dx.doi.org/10.1016/j.apor.2016.10.010

Zhao, M., & Cheng, L. (2014). Two-dimensional numerical study of vortex shedding regimes of oscillatory flow past two circular cylinders in side-by-side and tandem arrangements at low Reynolds numbers. *Journal of Fluid Mechanics*, 751, 1-37.

Zhou, H., & Wan, D. C. (2015). Numerical investigations on the aerodynamic performance of wind turbine: Downwind versus upwind configuration. *Journal of Marine Science and Application*, 14(1), 61-68.